Infill well evaluations of Jonah Field tight gas: characterization and simulation of complex architectural elements

Reinaldo J. Michelena,[1*] James R. Gilman,[1] Omar Angola,[1] Mike J. Uland[1] and Ira Pasternack[2]

This paper summarizes recent reservoir characterization and simulation studies performed in the Jonah Field, one of the most prolific natural gas fields in the Rocky Mountain region of the United States. The goal of the studies was to integrate geology, petrophysics, 3D seismic, and engineering data into 3D geologic and engineering models to evaluate infill well development in different regions of the field. This article shows how variations in channel development and thickness have a direct impact on gas recovery and optimal well spacing for different areas of the field. We also show that these channels can be mapped with the help of attributes inverted from pre-stack seismic data.

The following activities were performed for each study: petrophysical modelling for minerals, effective porosity, and fluid saturations, log and seismic based interpretation of markers, calibration with cores, generation of log-based facies proportions curves, pre-stack seismic inversion, estimation of seismic-based facies probabilities, and 3D geomodel construction. Multi-well reservoir simulations attempted to address long-term well performance including possible interference effects and optimal spacing. Pressure depletion seen at new infill wells was used to validate geologic models. Our results show that geologic factors have distinctive effects on long-term recovery in different regions of the field.

Jonah Field

Jonah Field is located in the Green River Basin in Sublette County, Wyoming, in the United States, and is estimated to contain 8 to 15 Tcf (2 x 10^{11} to 4 x 10^{11} m^3) of natural gas in a productive area of approximately 32 square miles (Figure 1). Most of the production of Jonah Field comes from overpressured and ultra low permeability sandstones of the Upper Cretaceous (Maestrichtian) Lance Formation. The Lance Formation is comprised of braided to meandering fluvial channels intercalated with overbank or floodplain siltstones and mudstones. Median permeability of sandstones within the Lance Formation is about 0.01 md and median porosity is about 8%. Due to the low permeability, stimulation is required to achieve economical production rates (Wolhart et al., 2006). Overpressure is also critical for the field economics since it helps to increase storage, preserve porosity and permeability, and increase relative permeability. Top of the Lance Formation ranges between 8000 - 10,000 ft and gross pay interval ranges between 2800 - 3500 ft. Significant changes of sandstone occurrence and thickness in closely spaced wells provide strong evidence for a high degree of vertical and lateral depositional compartmentalization in the Lance Formation. Strong compartmentalization translates into infill well performances that are highly variable and difficult to predict. For this reason, a reliable estimation of the facies distribution within the Lance is crucial for the development of the field. More details about Jonah Field can be found in a classic compilation of papers by Robinson and Shanley (2004).

Facies characterization and modelling workflow

The workflow utilized to characterize any reservoir depends on the available data, the geological problem to be addressed, the timeframe of the study, and the business question that such study is intended to answer. For Jonah Field, a workflow was devised to characterize facies using core data from different wells throughout the field, well logs from about 40–50 wells per study area, 3D post-stack and pre-stack seismic data, and check shots to facilitate seismic-well calibration. Three to four months was a typical timeframe for each study.

Characterization of the facies geometry focused on the identification of pay and non-pay facies using core and well log data. Pay facies consists of single and multi-story channels. Single story channels correspond to sandtone bodies accumulated in point bars associated with meander belts aligned in the NW-SE direction. Non-pay facies consist of floodplains, fine-grained shaly sandstones, and thin sandstones. These last two facies are interpreted to be small crevasse-splays and levees.

[1] *iReservoir.com, 1490 W. Canal Court, Littleton, CO 80129, USA.*
[2] *EnCana Oil & Gas (USA), 370 17th Street, Suite 1700 Denver, CO 80202-3950, USA.*
**Corresponding author, E-mail: michelena@ireservoir.com*

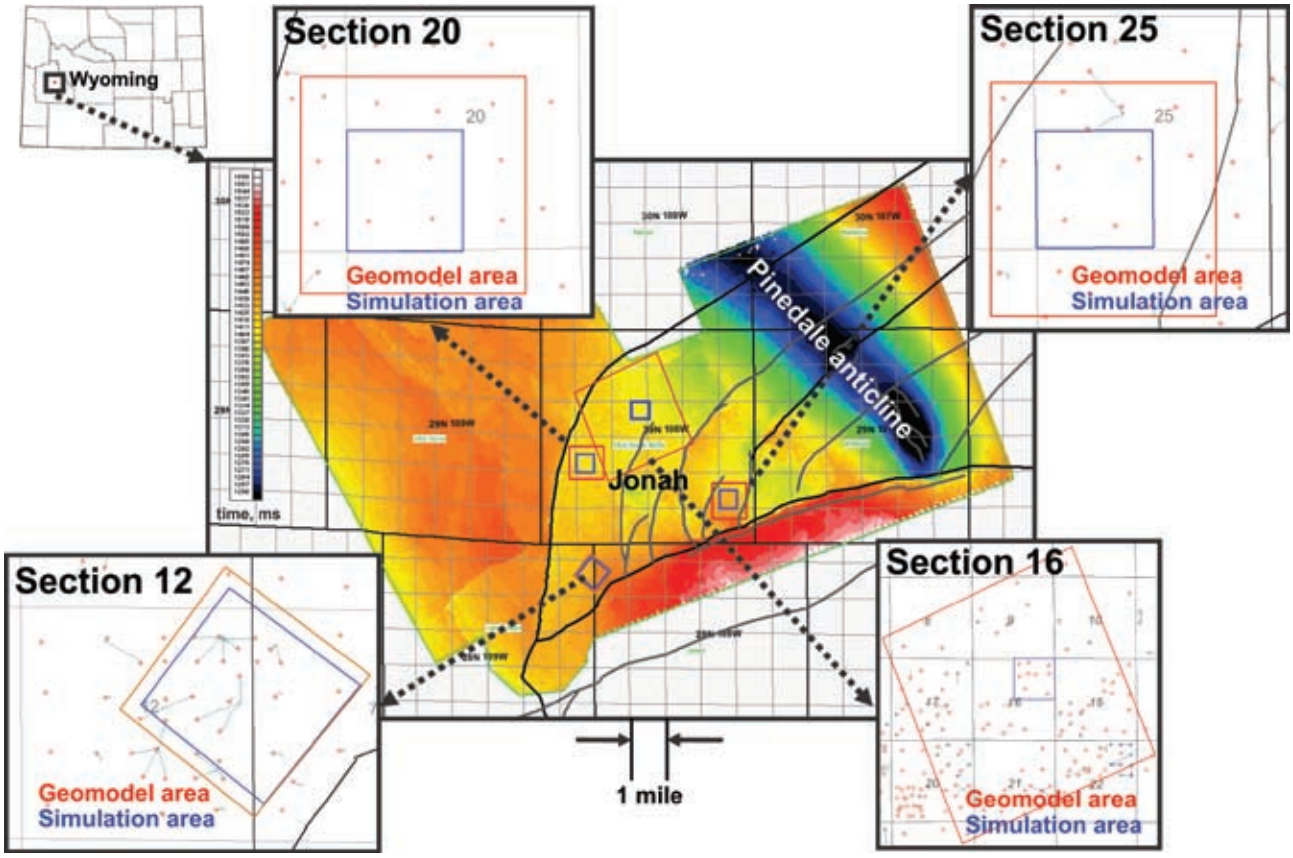

Figure 1 *Jonah Field location, structural map, and study areas. Jonah is defined by the intersection of two sub-vertical fault zones that form a wedge-shape structural block. Characterization and simulation efforts presented in this paper focus on four different sections within the main Jonah area. Detailed geomodels were built for each of the areas and reservoir simulation models were extracted from the larger geomodel areas. The area of one section is one square mile.The average area covered by each simulation model (in blue) was one quarter section (0.65 km^2). Sections and townships (36 sections) are the way public lands are usually divided in the United States. Unit conversion: 1 mile = 1.6 km.*

Facies geometries were characterized using three different methods to capture different scales and variability across each area: a) Local facies curves that capture the facies variability at each well location; b) Vertical proportion curves, that capture the global vertical facies variability for a whole area (one square mile, for instance); and c) Seismic driven facies probability cubes, that capture the spatial variations in facies distributions and are used as soft constraint when integrating all the facies information into a single geomodel. Local facies curves and vertical proportion curves are treated as hard data when building the geomodel.

Petrophysical analysis and modelling were the starting point of the reservoir characterization workflow in all areas of interest. Well logs may contain erroneous values in different zones along the wellbore that must be corrected before using them for further analyses. The result of the petrophysical modelling was a normalized set of enhanced logs used for seismic-well calibration, stratigraphic interpretation, and facies classification. Other products of the petrophysical modeling were estimates of shale volume, water saturation, porosity, and fractions of other minerals suspected to be present in the rocks of the area. Well-log derived porosities were calibrated with core data.

Determination of lithology and facies associations were the next steps after petrophysical analysis and modelling. A set of rules designed to classify all lithologies (coal, shale, silty shale, shaly sandstone, and clean sandstone) based on density and Vshale logs was applied to all wells. Results were carefully checked for misclassifications and calibrated with core data. Using these lithology logs, facies associations were then developed based upon the dominant lithology and thickness of each interval. Three facies were identified depending on the thickness of the clean sand interval: multi-story channels, single story channels, and silty-sandy floodplains (from thickest to thinnest, respectively). The term shaly floodplain was applied to non pay intervals where shales and/or coals were the dominant lithology. Figure 2 shows an example of the core-to-log calibration for facies classification at each well location.

Stratigraphic correlations and seismic interpretation are very difficult at Jonah Field due to rapid lateral changes

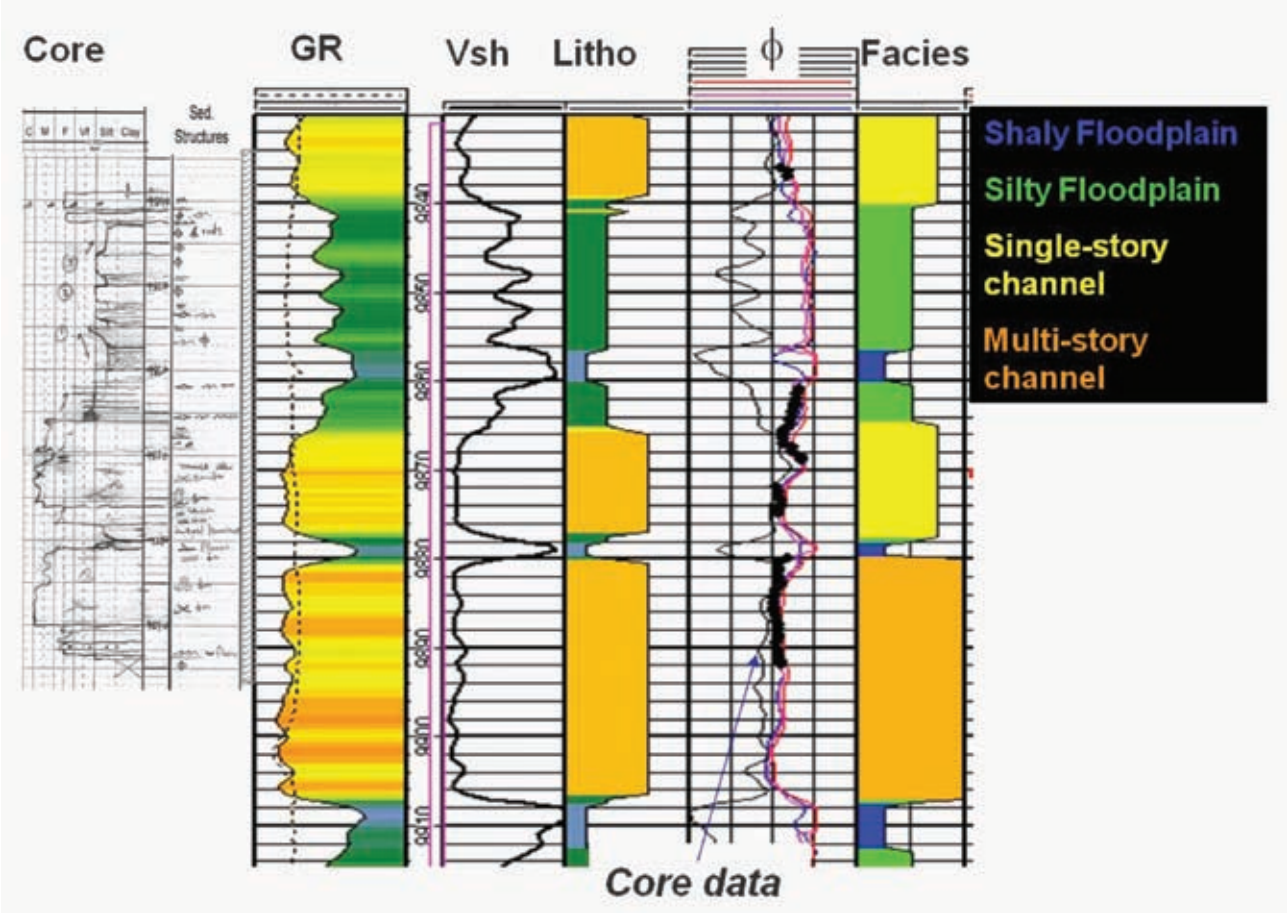

Figure 2 *Core-to-log calibration for generation of facies curves at each well location. Volume of shale curves (Vsh) are generated from petrophysical modelling of raw log data. Vsh curves and density curves are then grouped into five lithologies (coals, clean sandstones, shaly sandstones, silty sandstones, and shales) following a set of rules on each log calibrated with core data. Further grouping of lithology logs depending on the thickness of individual lithologies results in facies logs. Core data are also used to validate porosities and aid calibration of different facies. Units: depths range from 3000 m to 3021 m.*

in lithology within the Lance Formation. A variety of seismic attributes were examined to identify seismic events that were continuous within the different study areas. After interpreting events that looked continuous in any attribute extracted from the seismic data, check shots and sonic logs were used to convert these events to depth and use them as a framework to guide the stratigraphic correlation. Stratigraphic correlations were performed using lithology and facies logs obtained previously. After several iterations between stratigraphic correlations among different wells and careful seismic interpretation (usually performed in line-by-line fashion), a set of seismic horizons and well markers that were totally consistent with each other was obtained. The seismic horizons were also used as a guide to pick additional well markers that were not visible in the log data.

Once the seismic-guided stratigraphic correlations were completed, the Lance interval was divided into a fixed number of layers within each stratigraphic interval for all wells in each study area. Layer thickness was variable, but averaged approximately 5 ft. The total thickness of each facies for all wells was calculated for each layer and the relative proportions of the different facies by layer were computed. The results of this process are shown in Figure 3. These curves are known as 'facies proportion curves' and are used to estimate and constrain the relative amounts of each facies in each layer of the geomodel. From left to right, the plot for three different model areas shows the relative proportion of shaly floodplains, sandy floodplains, single-story channels, and multi-story channels respectively. After examining the relative proportions for each area, it is evident that in terms of spatial variability, section 12 is the most variable followed by sections 20 and 25, respectively. In terms of net-to-gross ratio of pay vs. non pay intervals, section 25 shows the higher values followed by sections 20 and 12 respectively. In other words, channels in section 25 show more continuity and higher net-to-gross ratios than channels in the other two sections. As will be shown in the reservoir simulation section below, these differences in channel variability and thickness have a direct impact on gas recovery for the different sections.

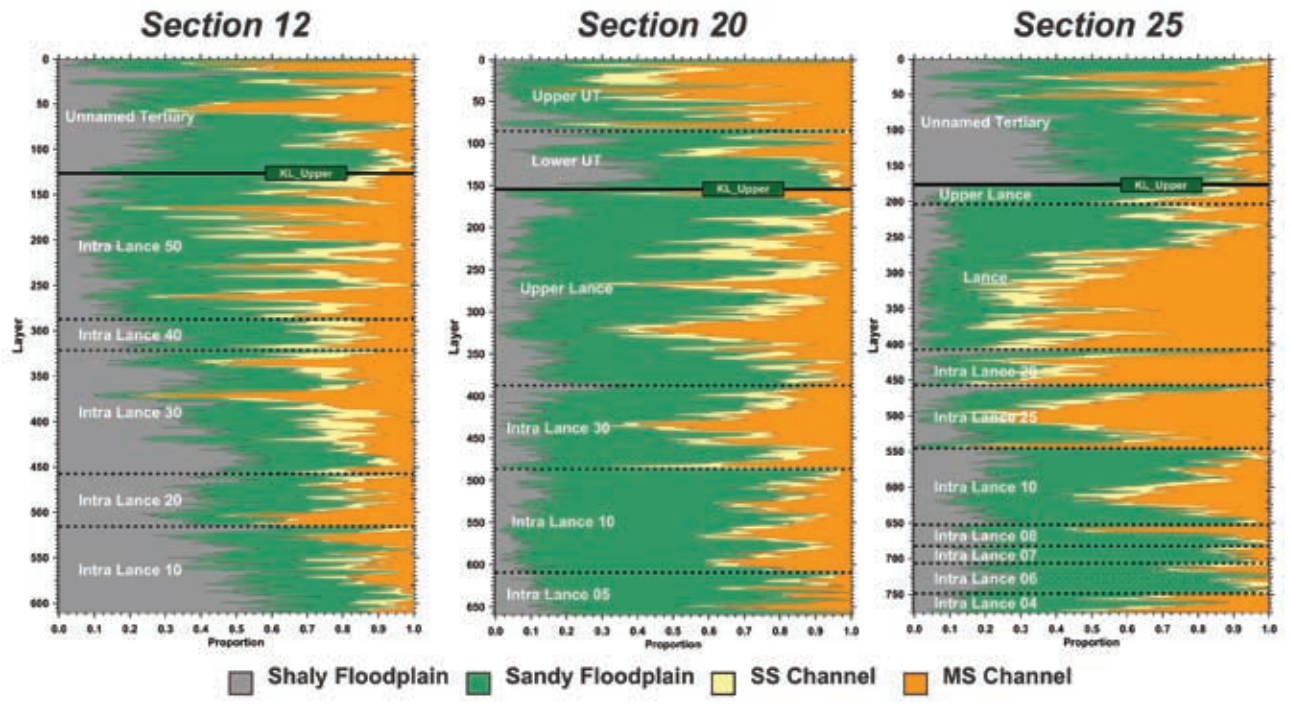

Figure 3 *Proportion curves of facies associations (commonly referred to as vertical facies proportion curves) for three different areas in Jonah Field. Numbers on the left indicate stratigraphic layers, and each layer is about 5 ft in average thickness. Each plot summarizes the facies information of approximately 40 wells in each area. The curves represent the cumulative proportion of each facies association, from left to right: shaly floodplain, sandy floodplain, single-story channel, and multi-story channel. Notice how the variability and thickness of facies is different from one area to the other. These differences have an important influence in the gas recovery of the different areas.*

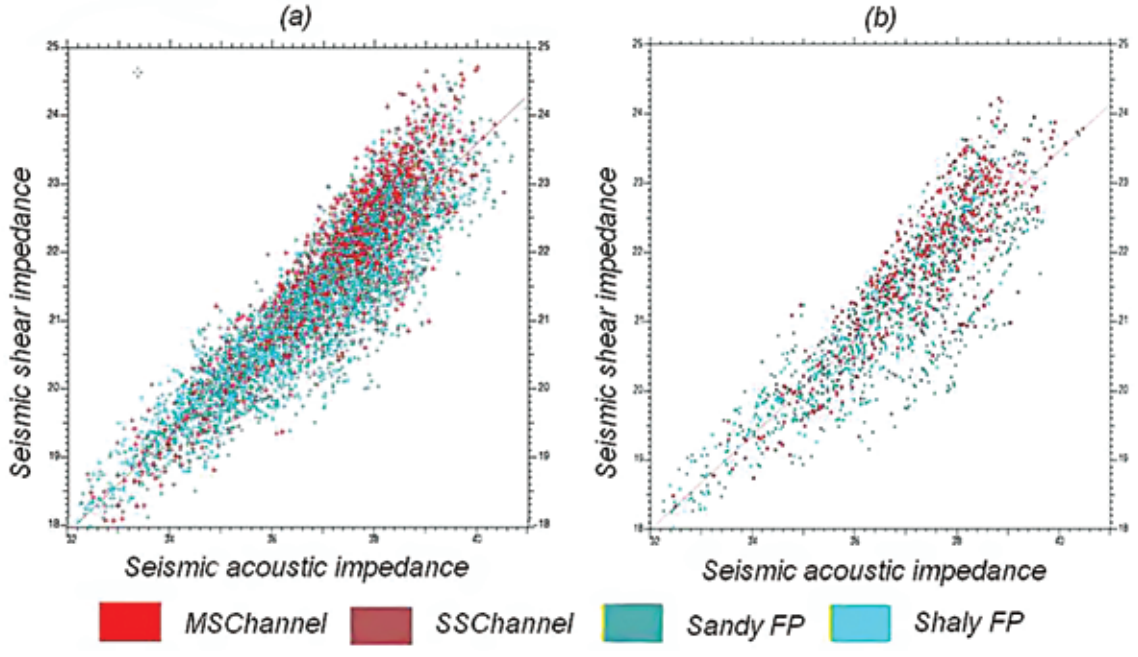

Figure 4 *Crossplots of seismic-scale acoustic and shear impedance extracted at (a) 39 and (b) four well locations in one of the sections studied at Jonah Field. The colours are the log scale facies at each well location. Acoustic and shear impedances were estimated by inversion of pre-stack seismic data. Depth converted impedances were sampled at each well location for the unnamed Tertiary and Lance intervals, The average thickness for these two intervals in the area of interest is about 3500 ft which means that the crossplot (a) generated using 39 wells contains approximately 300,000 points, more than enough to perform reliable statistical estimations. Notice that in both cases channel facies fall in the area of the crossplots that correspond to high impedance and low Vp/Vs ratios. These results show that at seismic- scale it is possible to separate channels facies from other facies at Jonah Field, even if the number of wells used for calibration is small.*

Rock physics analysis of well log data indicate that seismic attributes derived from 3D pre-stack seismic data may provide good indicators of the presence of channels in the Lance Formation. This observation served as the basis to justify performing acoustic and shear impedance inversion in a 100 square mile area in the middle of the field. Impedance results were converted to depth by using a velocity model that precisely matched all well markers. After time-to-depth conversion, seismic-scale acoustic and shear impedances were extracted at each well location at well-log resolution. Figure 4 shows crossplots of seismic scale impedances colour-coded by facies flags at log scale for two different cases: a) using 39 wells and b) using four wells. As expected from the analysis of log scale impedances, channel facies (in red) tend to cluster in the area of the crossplot that corresponds to high impedances and lower values of $V_p/V_{s\ ratio}$ regardless of the amount of wells used to create the crossplot. This means that at seismic scale, it is also possible to separate channel and non-channel facies at Jonah Field. Thus, for one of the study areas, seismic data were used to further constrain the facies distribution in geomodels.

Probabilities of channels are computed using a Bayesian approach equivalent to computing the probabilities of each facies within individual, discrete regions in the acoustic vs. shear impedance crossplot. Using this approach, acoustic and shear impedance cubes in depth were converted into a channel probability cube for the areas of interest. Figure 5 shows depth slices within the Lance Formation extracted from the channel probability cubes created using 39 and four wells respectively. Both slices show similar trends, but the one extracted from the probability cube built with 39 wells estimates shows overall lower probabilities. The fact that probabilities estimated by calibrating with 39 or four wells are similar means that this technique can yield useful results in areas of the field with poor well control. Figure 6 compares the average probabilities (for 39 and four wells) computed for each stratigraphic layer in one of the study areas with the channel proportions calculated using wells in the same area. Notice that seismic derived probabilities follow the same trend of the channel proportion curve which shows that seismic probabilities can be used to constrain the distribution of facies in the geomodel. The fact that the probabilities estimated using 39 wells are closer to the actual proportions estimated from well data than the probabilities estimated with four wells indicates that adding more wells helps not only with more reliable statistics but also to obtain better absolute probabilities.

In one study area, facies information derived from well data and seismic data was used to constrain the facies distribution in the geomodel. Even though individual facies curves at well locations and vertical proportion curves

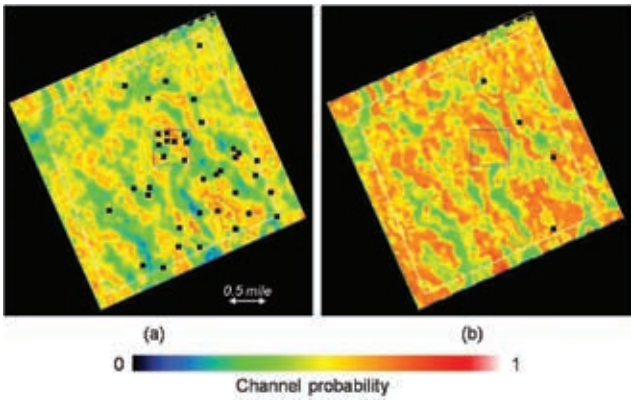

Figure 5 *Depth slices within Lance Formation of channel probabilities extracted from 3D channel probability cubes estimated from seismic-scale acoustic and shear impedances and log scale facies: (a) using 39 wells and (b) using four wells. Both slices are extracted at the same depth. Well locations used to compute the probabilities are shown in black. Both maps show similar trends, but the one created with four wells (b) tends to be more optimistic since these particular wells are located in a region of the field with higher overall sand content. A detailed reservoir simulation model was built in the area within the blue square. Unit conversion: 0.5 mile = 0.8 km.*

from a group of wells sample details of the vertical variability within the reservoir, they are not adequate to constrain the horizontal variability. On the contrary, as shown in Figures 5 and 6, 3D seismic data provide a better characterization of the horizontal variability than well-log derived information but samples the vertical variability poorly when compared to log data.

The first step of the geomodeling process consisted of selecting stratigraphic tops (constrained by geologic and geophysical integration) which were gridded to create the structural surfaces using seismic horizons as a guide. Second, a high-resolution 66 x 66 x 5 ft 3D stratigraphic grid was constructed to model the fine-scale vertical heterogeneity of the reservoir. After the grid was built, indicator-based simulation techniques were used to distribute facies in 3D. Experimental variograms were estimated from seismic-derived facies probability cubes wherever these probabilities were available. For the seismic constrained modelling, a rescaled version of the channel probability cube from seismic was used to constrain the lateral distribution of facies. Figure 7 shows the result of the facies distribution in 3D for selected layers of the model for one of the study areas. Notice how the facies distribution honours the facies proportions calculated from well data and reflects the heterogeneous nature of the fluvial environment.

Porosity was distributed using facies-dependent variograms and sequential Gaussian simulation while also honouring log data at the wells and porosity statistics per facies. Porosity in non-pay facies was set to zero. Water saturations were populated utilizing a core- and log-derived bulk-volume water (BVW) approach to satura-

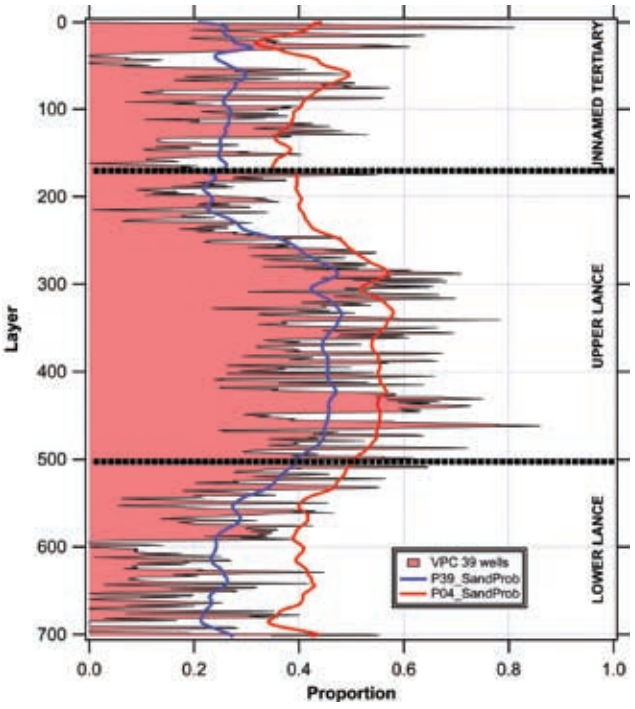

Figure 6 *Channel facies from vertical proportion curve (VPC) computed from 39 wells vs average channel probabilities extracted from seismic-derived facies probabilities estimated with 39 wells (blue) and four wells (red). Seismic derived probabilities follow the same trend of the VPC. The average layer thickness for the VPC is 5 ft.*

tion distribution. Permeability was distributed using a core-derived porosity-permeability cloud transform. Figure 8 shows the result of the porosity and permeability modelling. Notice that variations in permeability do not mimic exactly the variations in porosity. The reason for these differences is that the relation between the two parameters in the geomodeling was based on a non-linear statistical relation as defined by the cloud transform. For flow simulation, the fine-scale model was upscaled to preserve the vertical heterogeneous channel distributions and property variations.

Reservoir simulation in detailed geological models

The multi-well simulations performed for this project attempted to address long-term well performance including well interference effects and optimal spacing. Only minimal upscaling of the geologic model was undertaken for simulation in order to preserve the complex architectural elements. It was found to be important to maintain detailed geologic descriptions throughout the model area rather than using coarse grids with near-well refinements as is commonly applied. Long-term interference effects were more of a concern than short-term detailed rate profiles as would be required for optimizing hydraulic fracture treatments. The base input model was a result of three geostatistical realizations which were averaged.

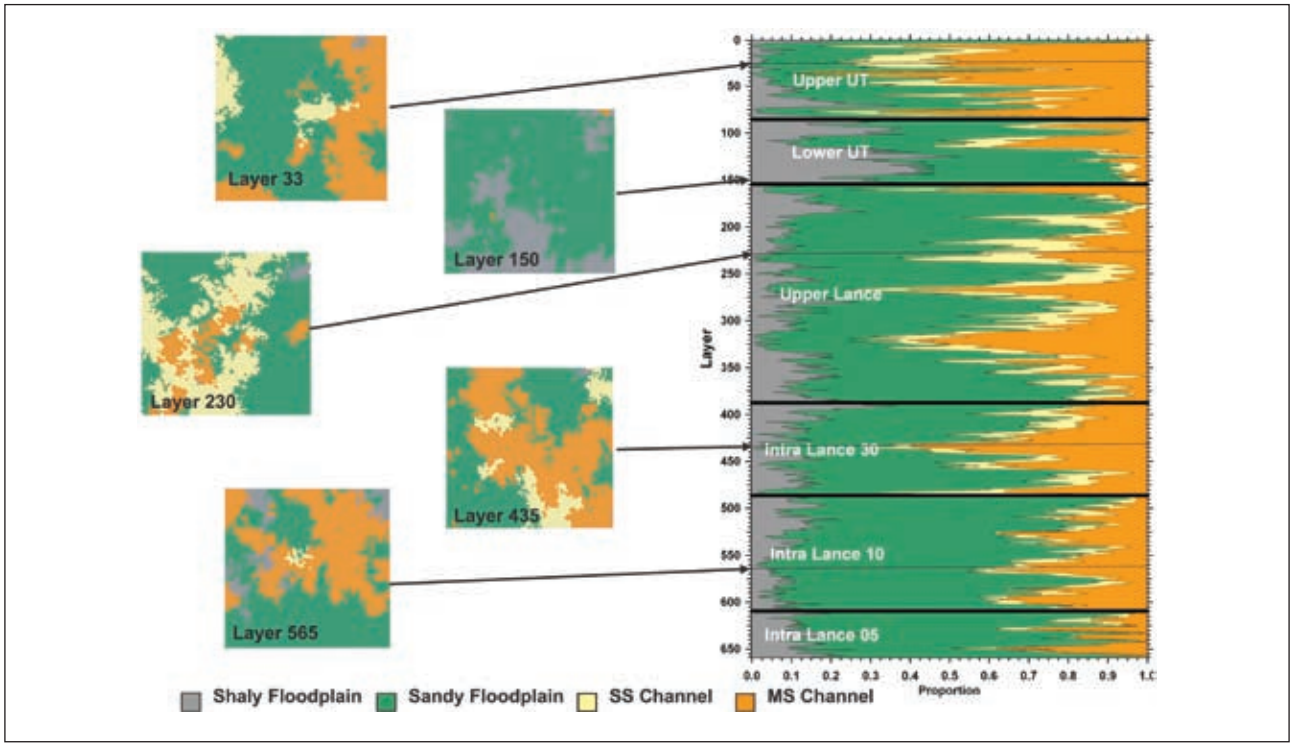

Figure 7 *Facies distribution in 3D for one of the study areas. The right figure is the vertical proportion curve while the left diagrams are map views of particular stratigraphic slices. Note that the facies distribution honours the facies proportions calculated from well data and individual layers reflect the heterogeneity of the fluvial environment. Information at individual wells is honoured while the distribution between wells is controlled by geostatistical relations conditioned to seismic-derived channel probability information wherever possible.*

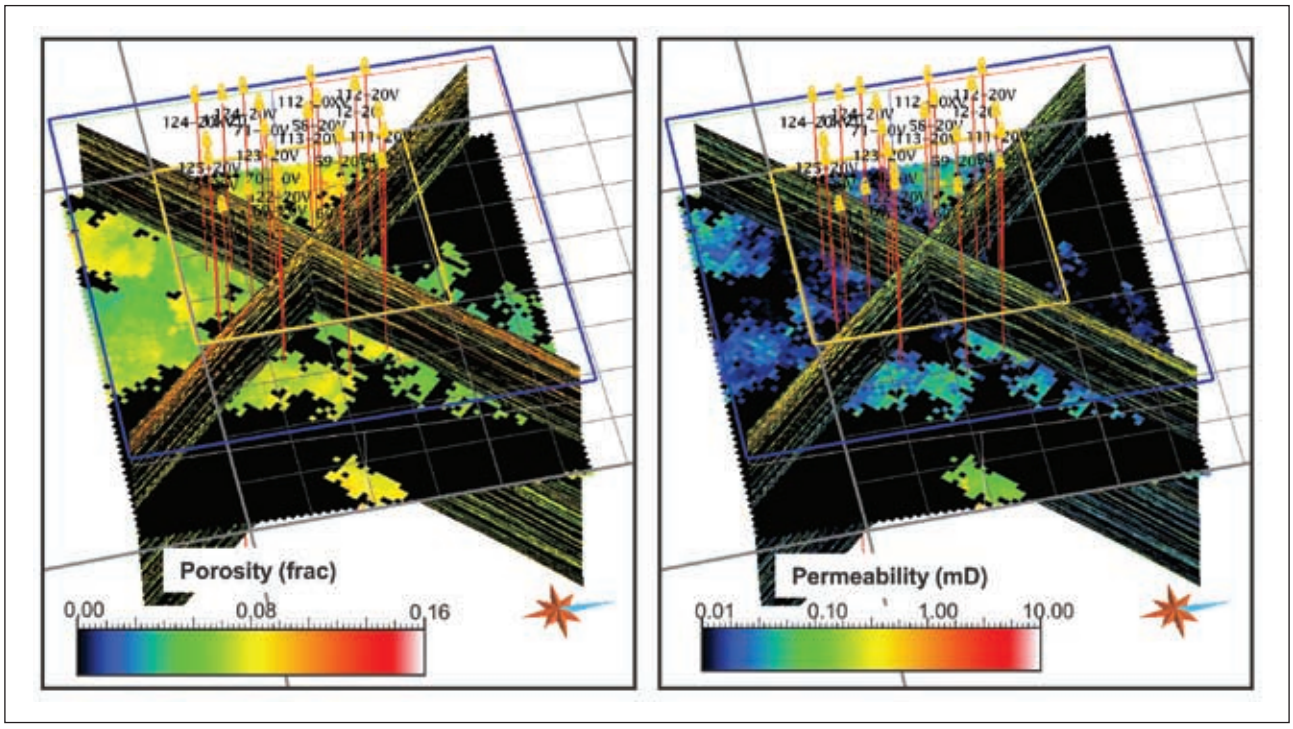

Figure 8 *Porosity and permeability distributed in pay facies. Porosity and permeability in non-pay facies was set to zero (black colouring). Porosity was distributed separately for each facies, honouring individual statistics and variogram. The permeability is based on a phi-k cloud transform and reflects core measured air permeability. For simulation, the core measured permeability is adjusted for overburden effects, water saturation, and gas slippage resulting in nearly an order of magnitude reduction in permeability compared to the values shown here.*

The assumption of irreducible initial water saturations was applied as determined from bulk-volume water relationships by facies. The presence of water has a significant impact on gas-in-place and the effective gas permeability (Shanley at al., 2004). In addition to using a gas permeability cloud transform based on core data to assign initial permeability values, core measured permeability was adjusted for overburden effects, water saturation, and gas slippage. These effects resulted in nearly an order of magnitude reduction in permeability compared to core data. Furthermore, utilizing laboratory measured compaction data, permeability loss was accounted for as pore pressure was reduced. This has important implications on long-term recovery (Lorenz at al., 1989). For pressure initialization, separate pressure regions were assigned according to defined stratigraphic intervals with initial pressures determined from the reservoir overpressure gradient. Pressure gradient may be as high as 1.16 psi/ft within the pay interval. Models were validated by matching tubing-head pressures while honouring historical gas rates. Models were also compared to historical production log data (PLT) and initial pressure profiles at infill wells (Figure 9). Pressure data were determined from diagnostic fracture injection tests (DFIT) or other direct pressure measurements. Many new infill wells show some level of pressure depletion. This has significant implications for optimal well spacing and was considered important data for model validation (Quint at al., 2006).

After model validation, forecasts were performed in which the simulator estimates future gas rates using tubing-head or bottom-hole pressure constraints. Simulated recovery factors and rate profiles provided information about well interference at 5 acre, 10 acre, 20 acre, and 40 acre spacing by running a selected number of predictions using existing and uniform well pattern locations. Simulations show that per-well recovery is reduced when comparing 40-acre to 5-acre spacing; however, total field recovery is increased as well spacing is reduced. For example, in section 20, 5 acre wells produce about 6.5% more gas at an economic limit compare to 10 acre wells and the recovery timeframe is reduced; however, per well recovery drops from about 2.6 to 1.4 Bcf (7.4×10^7 to 4×10^7 m^3). As mentioned previously, permeability loss from rock compaction was shown to have significant effect on long-term recovery. Model comparisons show the importance of maintaining the geologic detail when trying to access long-term recovery. The more continuous multi-storage channels in section 25 result in more efficient long-term drainage with 5 acre and 10 acre wells as compared with section 12 and 20. Comparisons of long-term recovery for uniform well spacing are shown in Figure 10.

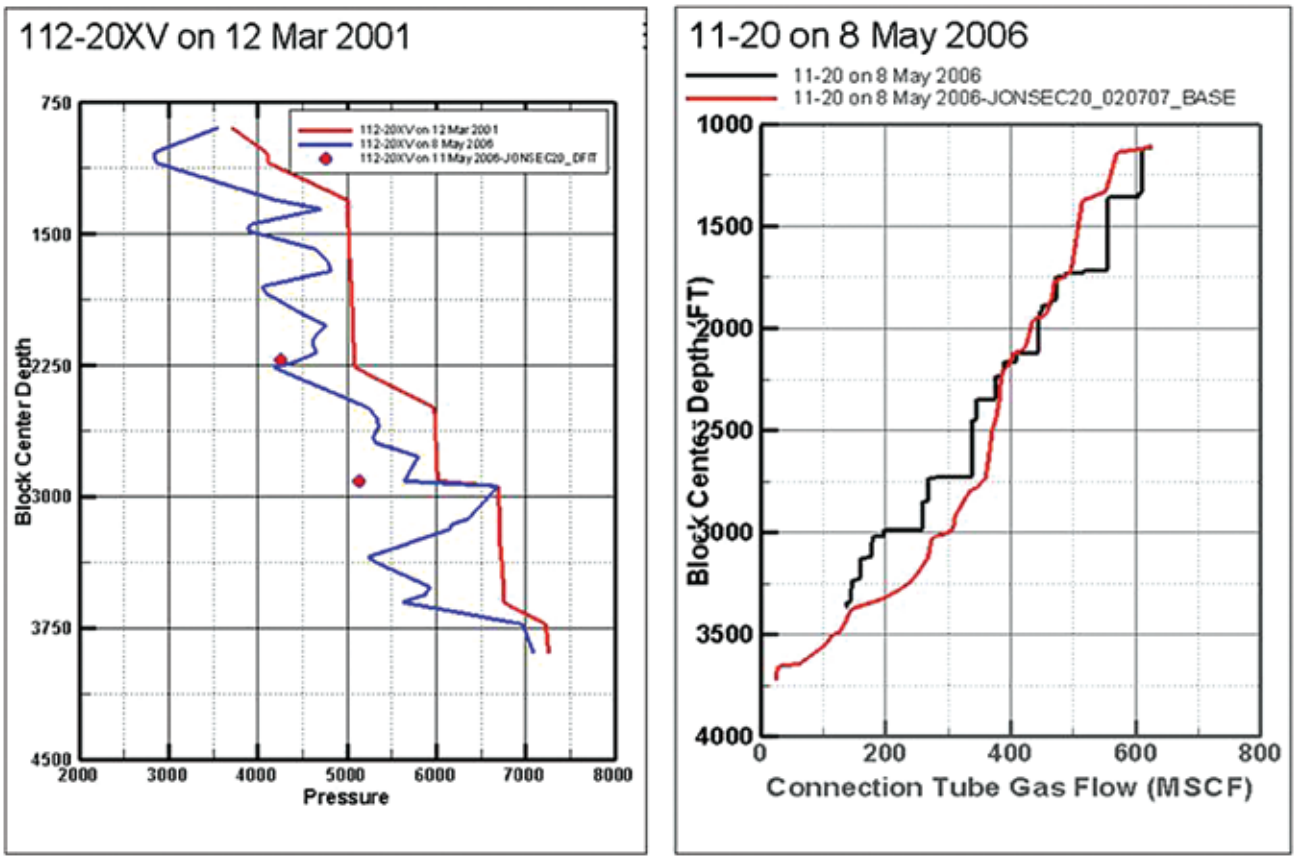

Figure 9 *In addition to validating the models by matching tubing-head pressures, models are also compared to initial pressure profiles and production log data (PLT) at infill wells. The pressure data are estimated from diagnostic fracture injection tests (DFIT) or other direct pressure measurements. In the figure on the left, the simulated depletion data at a recent infill well (blue vs. red line) is similar in magnitude to the measured pressure depletion (symbols) providing confidence in the geologic models. Pressure depletion has significant implications for optimal well spacing. Measured production inflow (black line on left) was also approximated by the simulator (red line) providing confidence in the hydraulic fracture assumptions. Unit conversion left figure: depths range from 229 m to 1372 m and pressures range from 13789 Kpascal to 55158 Kpascal. Unit conversion right figure: depth ranges from 305 m to 1219 m and gas flows range from 0 standard cubic metres (scm) to 22653 scm.*

Discussion and conclusions

The Lance interval shows large variations in proportion of pay intervals across the field as shown by the detailed reservoir characterization of the separate areas described in this paper. These variations will have a considerable impact in the development plans and economic forecasts. Drilling patterns adequate for one area may be inadequate for others which means that the same drilling recipe cannot be applied to the whole field.

Seismic data can be used to separate channel facies from other non-producing facies in this tight gas reservoir provided well control is 'representative' of acoustic properties of the rocks. Adding more well control increases the reliability and accuracy of channel probabilities estimated from seismic data. Since seismic-derived channel probabilities show similar trends as the proportions of channels derived from well data only, seismic data can be used to help prioritize areas of the field with respect to presence of channel and potential connectivity of channel facies. Seismic data can also be used to help in the construction of better geomodels by introducing lateral variability and developing more reliable variograms.

The reservoir simulations show that matches to historical gas rate decline were consistent with the integrated static and dynamic data providing confidence in the methodologies applied. The models incorporate well completion information and were also consistent with production logs and infill well pressure depletion data. The simulations show significant variability in incremental long-term recovery when going from 40 acre to 5 acre spacing. These comparisons show the importance of the integrated approach and detailed models for assessing long-term recovery. Some model areas showed nearly 10% incremental with the 5 acre development compared to minimal incremental recovery in other areas. The difference is largely attributable to differences in continuity and number of multi-storage channels; thus permeability and hydraulic fracture effectiveness are not the only issues with regard to infill drilling in tight gas reservoirs. More standard methodologies, such as decline curve analysis,

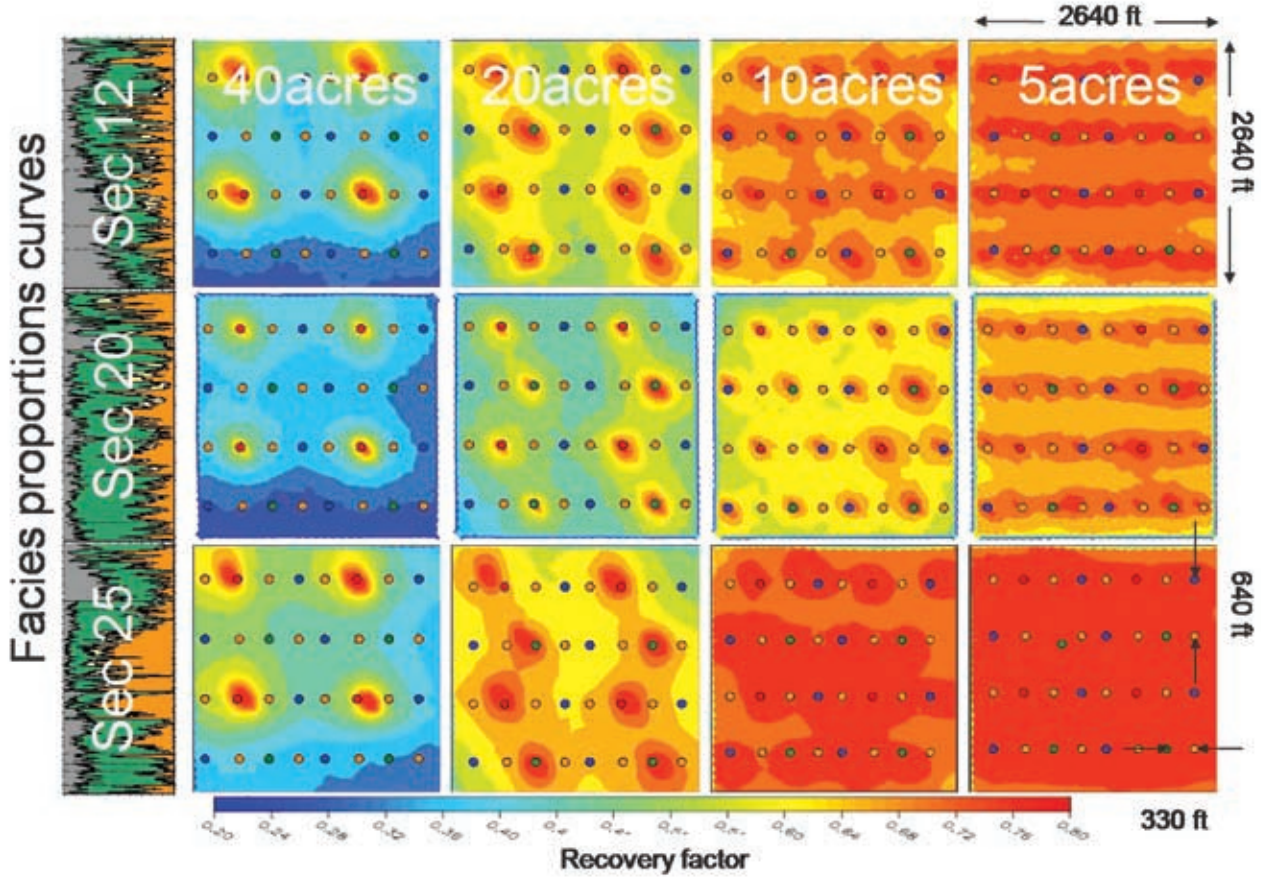

Figure 10 *Simulated long-term recovery maps for the various modeled areas and various well spacing assumptions. These maps show long-term recovery assuming uniform well spacing with all wells starting at the same time. A 5 acre well pattern is always shown, but not all wells are active. The well spacing is elongated NS relative to EW to allow for elliptical drainage in NW-SE direction based on maximum stress and depositional geometry. The left column shows the Jonah section number on top of the facies proportion curve. Well spacing varies from 40 acres to 5 acres going left to right. Blue represents 20% recovery of OGIP while red represents 80% OGIP. Note how the variations in recovery reflect the variations in the proportion curves. The detailed geologic models developed via an integrated characterization approach are important for accessing long-term recovery and optimal infill well spacing. Unit conversion: 2640 ft = 805 m; 640 ft = 195 m; 330 ft = 101 m.*

can provide misleading results with regard to optimum well spacing.

Successful reservoir characterization of this kind of geologically complex reservoir depends to a large extent on how diverse information is applied in a manner that is both consistent and complementary. Details are important and numerous iterations between disciplines may be required to ensure data consistency.

Acknowledgements

We thank EnCana Oil & Gas USA for permission to publish this paper. We also thank Juan Florez (now with BP), Carolyn Fleming (now with Shell), Nancy House (EnCana Oil & Gas USA), and Richard Merkel (now with Newfield Exploration), for their important contributions to this work. A shorter version of this work was already published in the *American Oil and Gas Reporter.* Thanks for it permission to use part of that material in this new, expanded publication.

References

Lorenz, J.C., Sattler, A.R., Stein, C.L. [1989] The effects of depositional environment on petrophysical properties of Mesaverde reservoirs, Northwestern Colorado. *SPE Annual Technical Conference & Exhibition,* SPE 19583.

Quint, E., Singh, M., Huckabee, P., Brown, D., Brake, C.B., Bickley, J. and Johnston, B. [2006] 4D pressure pilot to steer well spacing in tight gas. *SPE Annual Technical Conference & Exhibition,* SPE 102745.

Robinson, J.W. and Shanley, K.W. (Eds) [2004] Jonah Field: Case study of a giant tight-gas fluvial reservoir. *AAPG Studies in Geology*, **52**, *and Rocky Mountain Association of Geologists 2004 Guidebook*.

Shanley, K.W., Cluff, R.M. and Robinson, J.W. [2004] Factors controlling prolific gas production from low-permeability sandstone reservoirs: implications for resource assessment, prospect development and risk analysis. *AAPG Bulletin,* **88**(8), 1083-1121.

Wolhart, S.L., Harting, T.A., Young, T.J., and Mayerhofer, M.J. [2006] Hydraulic fracture diagnostics used to optimize development in Jonah Field. *SPE Annual Technical Conference & Exhibition*, SPE 102528.